A Molecular Dynamics Simulation Study of Polymer Dynamics in Aqueous Poly(ethylene oxide) Solutions

Oleg Borodin, Dmitry Bedrov, and Grant D. Smith*

Department of Materials Science and Engineering and Department of Chemical and Fuels Engineering, University of Utah, 122 S. Central Campus Drive, Rm. 304, Salt Lake City, Utah 84112

Received January 8, 2001; Revised Manuscript Received May 15, 2001

ABSTRACT: We have performed molecular dynamics simulations of aqueous solutions of poly(ethylene oxide) (PEO) in order to investigate the influence of water on polymer dynamics as a function of solution composition. Simulations were performed on 12 repeat unit PEO chains (530 Da) at 318 K covering a composition range (polymer weight fraction w_p) from 0.17 to 1.0. It was found that addition of a small amount of water to a PEO melt dramatically affects polymer dynamics on all length scales, leading to a maximum in relaxation times in the range $w_p = 0.78-0.90$, with the greatest effect occurring for smaller length-scale motions. With further dilution relaxation times decreased dramatically, with the greatest effect occurring for the largest length-scale motions. Water slows the rate of conformational transitions in PEO compared to the melt, an effect that sets in rapidly with initial dilution and saturates at $w_p \approx 0.5$. Initial addition of water leads to an increase in the heterogeneity of the rate of conformational transitions, with a maximum in the range $w_p = 0.78-0.90$, followed by a decrease in heterogeneity with further dilution. A maximum in the non-Gaussianity of PEO atom displacements was observed in the same composition range. On the segmental scale, water was found to engender a monotonic decrease in relaxation anisotropy and an increase in the efficacy of conformational transitions in effecting PEO segmental relaxation. Finally, water was found to first lead to a slight increase and then to a dramatic decrease in the longest relaxation times of the solution, including viscosity, with dilution.

I. Introduction

Poly(ethylene oxide) (PEO) is an amphiphilic polymer exhibiting lower critical solution temperature behavior (LCST) in many solvents including methyl, ethyl, and *n*-propyl alcohol as well as acetone and both LCST and upper critical temperature (UCST) behavior in water and *tert*-butyl acetate.[1] Phase-separated mixtures of PEO with other polymers such as dextran are used for protein purification.[2] Other applications of PEO include protein crystallization,[3−5] modification of surfaces[6,7] for biocompatibility, control of particle aggregation in solution,[8,9] modification of natural and artificial membranes,[10,11] and aqueous biphasic separations.[12] Due to the widespread importance of PEO in aqueous solutions, we[13−17] and other groups[18−22] have conducted molecular dynamics (MD) simulation studies of ether/water and PEO/water solutions in order to gain atomistic level insight into the thermodynamics and dynamics of PEO and its oligomers in aqueous solution. In our previous work[14] we demonstrated the ability of MD simulations using our quantum-chemistry-based force field to accurately predict viscosity,[13] water self-diffusion coefficients,[15,17] excess volume,[13] and changes in 1,2-dimethoxyethane (DME) conformations[14] with composition in DME/water solutions. The self-diffusion coefficient of water and its temperature dependence in PEO/water solutions[23] were also accurately reproduced. We also have demonstrated that inaccurate descriptions of water/ether and ether/ether interactions can lead to serious discrepancies between simulations and experimental results.[14]

Our recent simulations demonstrated a complex dependence of PEO conformations,[24] chain dimensions,[24] and the extent of water−water and ether−water hydrogen bonding[25] on solution composition and temperature. Here, we investigate polymer dynamics in PEO/water solutions in order to determine how the complex dependence of static properties on solution composition is carried over to dynamical properties. In a future paper we will consider the composition dependence of water dynamics in PEO/water solutions and address the influence of temperature on polymer and water dynamics.

II. MD Simulation Methodology

A quantum-chemistry-based force field for ether/ether[26] and ether/water interactions[13] together with the transferable intermolecular four-point potential (TIP4P) model for water[27] was used in our simulations. MD simulations were performed on aqueous solutions of 12 repeat unit PEO chains $H-(CH_2-O-CH_2)_{12}-H$ for compositions (polymer weight fraction) $w_p = 0.17$, 0.35, 0.52, 0.65, 0.78, and 0.90 and pure PEO melts at 318 K and for $w_p = 0.52$ at 298 K. The simulation box consisted of approximately 4000 atoms with 8−32 PEO chains depending on composition. The Ewald summation method[28] was used to calculate long-range Coulomb interactions. Bond lengths were constrained using the Shake algorithm.[29] A cutoff radius of 10.0 Å was used for dispersion interactions. Simulations of 0.5−2.0 ns were performed in an NPT ensemble using the velocity Verlet algorithm[28] to establish solution densities at 1 atm pressure. Those densities were used in NVT simulations employing a multiple time step reversible reference system propagator algorithm[30,31] with a time step of 0.7 fs for bonding, bending and torsional motions, with a 1.4 fs time step for nonbonded interactions within a 6.5 Å sphere, and a 2.8 fs time step for nonbonded interactions between 6.5 and 10.0 Å and the reciprocal space part of the Ewald summation. Production runs were 20−50 ns.

10.1021/ma010038b CCC: $20.00
Published on Web 07/07/2001

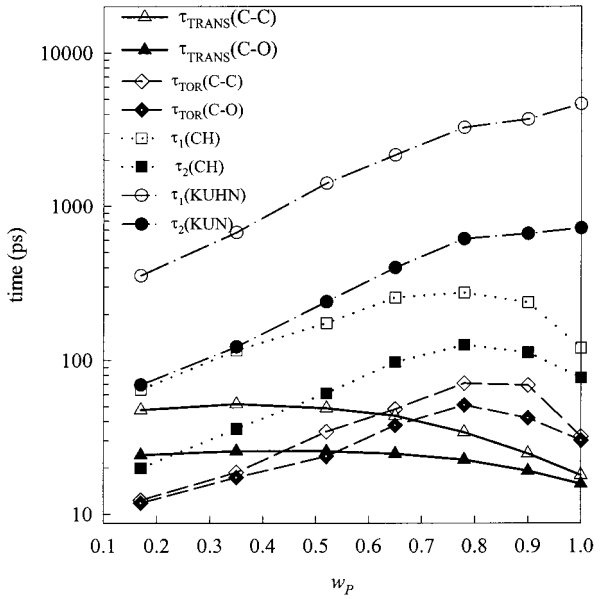

Figure 1. Mean conformational transition and autocorrelation times as a function of solution composition.

III. Conformational Transition Rates

A. Mean Conformational Transition Rates. Polymer motion on all length scales is fundamentally related to conformational dynamics. Therefore, we begin our study of polymer dynamics in PEO/water solutions by investigating the influence of water on the mean conformational transition times (τ_{TRANS}) shown in Figure 1 for C−C and C−O dihedrals. A conformational transition is considered to have occurred when the state of the dihedral ($0° \leq g^+ < 120°$, $120° \leq t < 240°$, $240° \leq g^- < 360°$) for the current configuration differs from that of the previous configuration. Analysis was performed on trajectories with configurations stored every 2 ps. The initial addition of water dramatically increases τ_{TRANS} for C−C and to a lesser extent for C−O transitions when compared to the neat melt. The influence of water on conformational transition rates largely saturates at $w_p \approx 0.5$; we do not observe any significant change in the rates of conformational transitions with further dilution. This behavior coincides with the saturation of ether/water hydrogen bonding at $w_p \approx 0.5$ observed in our previous simulations.[25] It is also at this composition that additional water no longer exclusively participates in perfecting the first hydration shell of PEO and begins to exhibit "pure water"-like behavior.[14,15]

B. Heterogeneity in Mean Conformational Transition Rates. In previous simulations of PEO melts, we observed that conformational dynamics, quantified in terms of the distribution of conformational transition rates, are quite heterogeneous on time scales comparable to the mean conformational transition time.[32] We have investigated the influence of water on heterogeneity in PEO conformational dynamics by monitoring the normalized dispersion in the distribution of the number of conformational transitions given by

$$\sigma^2_{TOR}(t) = \frac{\langle n(t) - \langle n(t)\rangle)^2}{\langle n(t)\rangle^2} = \frac{\langle r(t) - \langle r(t)\rangle)^2}{\langle r(t)\rangle^2} \qquad (1)$$

Here, $n(t)$ is the number of transitions a given dihedral has undergone during time t and $\langle\ \rangle$ denotes an ensemble average over all dihedrals of a given type. Equivalently, $\sigma^2_{TOR}(t)$ is the dispersion in the rate of conformational transitions $r(t)$, where $r(t) = n(t)/t$. $\sigma^2_{TOR}(t^*)$ for PEO/water solutions is shown in Figure 2 as a function of solution composition, where $t^* = t/\tau_{TRANS}$. Note that t^* is equal to the mean number of transitions $\langle n(t)\rangle$ that the dihedral has undergone after time t. Also shown in Figure 2 is the dispersion in a perfectly dynamically homogeneous system, i.e., a system in which all dihedrals exhibit the same rate of conformational transitions. For sufficiently large systems after a sufficient number of transitions, a homogeneous system will follow a Poisson distribution. The least dispersion in conformational transition rates (the most homogeneous conformational dynamics) is seen for pure PEO and $w_p = 0.17$, while the greatest heterogeneity is seen for $w_p \approx 0.78$. Note that while the mean transition rate is nearly independent of composition for $w_p < 0.5$ (Figure 1), the heterogeneity in transition rates continues to decrease with dilution in this composition range.

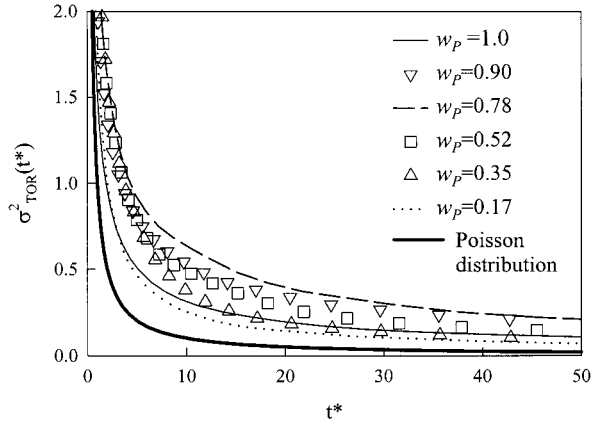

Figure 2. Dispersion of conformational transition rates $\sigma^2(t^*)$ for C−C dihedrals as a function of the mean number of conformational transitions.

IV. Conformational and Segmental Dynamics

A. Time Autocorrelation Functions. Water strongly influences the mean rate and distribution of rates of the fundamental microscopic polymer motion in PEO solutions, i.e., conformational transitions. It is of interest to see how the composition dependence of macroscopic relaxations, given by corresponding time correlation functions, and the composition dependence of these microscopic motions are related. In particular, we have investigated the torsional autocorrelation functions (TACF) for each type of dihedral, defined as

$$P_i(t) = \frac{\langle \cos(\phi_i(t))\cos(\phi_i(0))\rangle - \langle \cos(\phi_i(0))\rangle^2}{\langle \cos^2(\phi_i(0))\rangle - \langle \cos(\phi_i(0))\rangle^2} \qquad (2)$$

where $\phi_i(t)$ is the angle of a particular dihedral i at time t, and the ensemble average is carried out over all dihedrals of the same type, either C−C or C−O (O−C). In addition, we have investigated the behavior of several orientational autocorrelation functions (OACF), given as

$$P_1(t) = \langle [\mathbf{e}(t)\cdot\mathbf{e}(0)]\rangle \qquad (3a)$$

$$P_2(t) = 0.5[3\langle [\mathbf{e}(t)\cdot\mathbf{e}(0)]^2\rangle - 1] \qquad (3b)$$

where $\mathbf{e}(t)$ is a unit vector and $\langle\ \rangle$ denotes an ensemble average over all such vectors. In particular, we have investigated the C−H vector OACF and the OACF of statistical segments (Kuhn segments). The latter are defined as vectors connecting the atoms of a polymer chain separated by six bonds. The relaxation of the $P_2(t)$ C−H vector autocorrelation function is directly related to ^{13}C spin−lattice relaxation, which is well reproduced by our potential for PEO melts.[33]

As in our previous studies of PEO melts[33] and PEO/Li salt electrolytes,[32] we found that the decay of PEO TACFs for C−C and O−C dihedrals from 0.95 to 0.02 could be adequately described by a stretched exponential or Kohlrausch−Williams−Watts (KWW) expression given by

$$P_{\mathrm{KWW}}(t) = \exp[-(t/\tau)^{\beta}] \tag{4}$$

A reasonable representation of the P_2 OACFs was also possible for the same range of decay using the KWW expression. The P_1 OACFs were found to be well described by the modified KWW (MKWW) expression

$$P_{\mathrm{MKWW}}(t) = (1 - A)\exp[-(t/\tau)^{\beta}] + A\exp[-t/\tau_{\mathrm{TAIL}}] \tag{5}$$

for a similar range of decay. Here, the single-exponential term accounts for a long-time tail in the relaxation process not well described by the KWW expression. For a Debye relaxation process ($\beta = 1$), the macroscopic relaxation follows single-exponential behavior with a relaxation time given by τ. The stretching exponent β reflects deviation of the relaxation from Debye behavior. We can characterize a non-Debye process by the autocorrelation times τ_{TOR}, τ_1(OACF), and τ_2(OACF) defined as the time integral of the torsional, P_1, and P_2 OACFs, respectively. τ_{TOR} is the characteristic time over which all dihedrals of a given type will visit each conformational state with ensemble average probability, τ_1(CH) and τ_2(CH) are the time scales for rotational decorrelation of the C−H vectors, and τ_1(KUHN) and τ_2(KUHN) are the time scales for rotational decorrelation over the length scale of a statistical segment.

Autocorrelation times for the C−C and C−O dihedrals, the C−H vectors, and the statistical segment vectors, given by integration of the KWW or MKWW fits to the corresponding autocorrelation function, are shown in Figure 1 as a function of solution composition. The autocorrelation times either exhibit maxima in the composition range $w_{\mathrm{p}} = 0.78-0.9$ (dihedral and C−H vector) or saturate with polymer concentration for $w_{\mathrm{p}} > 0.78$ (statistical segment). The somewhat stronger composition dependence of τ_{TOR} for C−C dihedrals compared to C−O dihedrals is consistent with the greater influence of water on the rate of conformational transitions and conformational populations of the former.[24] Comparison of τ_{TRANS} with the autocorrelation times reveals that the composition dependence of the latter cannot be explained simply in terms of the composition dependence of the mean rate of conformational transitions. While it is reasonable to associate the increase in τ_{TOR} and τ(CH) with the decreasing rate of conformational transition with dilution in the range $0.78 < w_{\mathrm{P}} < 1.0$, the decrease in each of the autocorrelation times with dilution for $w_{\mathrm{p}} < 0.78$ is not associated with a corresponding increase in the rate of conformational transitions.

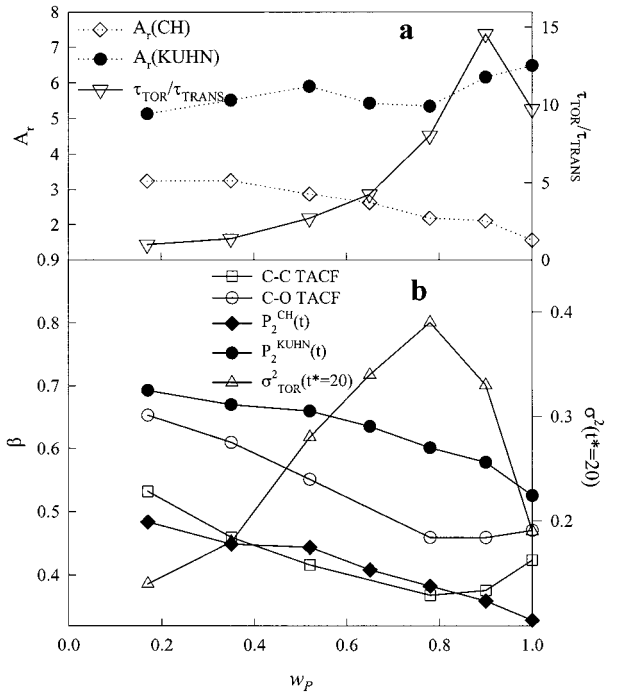

Figure 3. Anisotropy ratio A_{r} for C−H and statistical segment vector relaxation and the ratio of the torsional autocorrelation time to the average time of torsional transition for C−C dihedrals; $\tau_{\mathrm{TOR}}/\tau_{\mathrm{TRANS}}$ is shown relative to the ratio in the most dilute solution investigated. Also shown is the stretching exponent β as a function of solution composition for torsional, C−H, and statistical segment vector autocorrelation functions as well as the dispersion in conformational transition rates for the C−C dihedrals after 20 (mean) transitions per dihedral.

B. Non-Debye Relaxation Behavior. Figure 3 shows the values of the stretching exponent β obtained from the KWW fits to the torsional ACFs (eq 2) and the $P_2(t)$ OACFs (eq 3b) as a function of composition. The TACFs show greatest deviation from Debye behavior (smallest β) in the composition range $w_{\mathrm{p}} = 0.78-0.90$. In contrast, β for the OACFs functions increases monotonically with dilution within the uncertainty in the β values. Figure 3 illustrates that the composition dependence of $\sigma^2_{\mathrm{TOR}}(t^* = 20)$ closely corresponds to that of β for the TACFs but differs qualitatively from that of the β for the OACFs. The former agreement is a strong indication that the behavior of the TACF is tied to heterogeneity in the rate of individual conformational transitions. Indeed, in the composition range $w_{\mathrm{p}} < 0.5$, where the mean rate of conformational transitions is nearly independent of composition, the decreasing heterogeneity in the rate of conformational transitions is the most likely explanation for the decrease in τ_{TOR} with continued dilution, since by definition the TACF can decay only as result of individual conformational transitions. A simple two-state spin model demonstrates the influence of dynamic heterogeneity on correlation times. Figure 4 shows the autocorrelation function

$$P(t) = \langle s_i(t)\, s_i(0)\rangle \tag{6}$$

for an ensemble of uncorrelated spins ($s_i = +1$ or -1). In each of the three cases illustrated, the mean probability that a given "dihedral" (spin) undergoes a "transition" (a spin flip via a Monte Carlo move) per unit time is constant at 1/20. In other words, as in PEO/water solutions for $w_{\mathrm{p}} < 0.5$, the mean transition rate is constant. In the first case, each spin undergoes

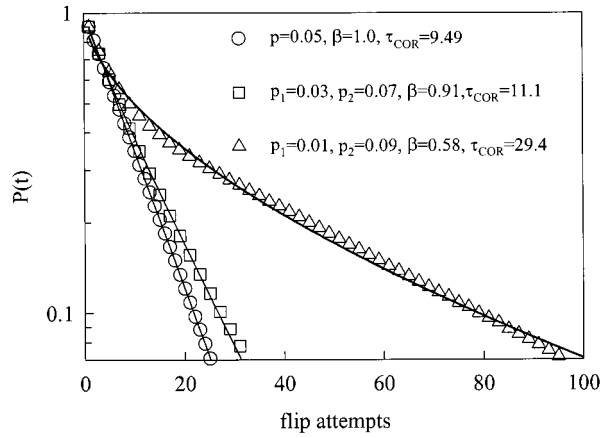

Figure 4. Autocorrelation function for an ensemble of uncorrelated spins. Lines are exponentials (homogeneous dynamics) and stretched exponentials (heterogeneous dynamics) fits to the simulation data. Correlation times τ_{COR} for each set of flip rates are also given.

transitions with the mean probability (a dynamically homogeneous system), yielding single-exponential decay of the autocorrelation function and a correlation time corresponding to the mean transition time. In the second and third cases, $^1/_2$ of the spins flip faster and $^1/_2$ flip slower than average. Figure 4 illustrates that the greater the dispersion in the transition rates, the longer the autocorrelation time and the smaller the β for the relaxation process.

A final illustration of heterogeneity in conformational dynamics can be found in Figure 3a, where the ratio τ_{TOR}/τ_{TRANS} is shown as a function of composition for both C−C dihedrals. Values are shown relative to the ratio in the most dilute solution investigated. The quantities τ_{TOR} and τ_{TRANS} sample conformational dynamics differently—the former is much more sensitive to dihedrals that exhibit slow dynamics.[34] In the same way that an increase in the ratio of the translational diffusion coefficient to the rotational diffusion coefficient of probe molecules in a polymer matrix (e.g., with decreasing temperature) indicates increasingly heterogeneous dynamics,[35] an increase in τ_{TOR}/τ_{TRANS} indicates increasely heterogeneous conformational dynamics. This ratio has a maximum in the composition range $w_p = 0.90$, consistent with the other measures of conformational heterogeneity.

The qualitative disagreement between the composition dependence of β for the OACFs and $\sigma^2_{TOR}(t)$ indicates that the relaxations of the C−H and statistical segment vector OACFs are at least partially decoupled from the dynamics of individual dihedrals. This disconnect is consistent with the fact that both the C−H and statistical segment vector reorientation occurs as the result of largely cooperative transitions of many neighboring dihedrals, whose combined dynamics are intrinsically more homogeneous than those of individual dihedrals. This is illustrated clearly by our recent simulations of random cis/trans/vinyl 1,4-polybutadiene melts where we observed more than an order of magnitude difference in the mean conformational transition rate depending upon the local chemical environment of the dihedral.[34] In contrast, for the same system different chemical environments resulted in at most a factor of 2 difference in correlation time for the various C−H vectors.

C. Relaxational Anisotropy. In polymer melts and solutions, the reorientation of local vectors occurs anisotropically, with motion perpendicular to the local polymer backbone occurring more rapidly than reorientation along the backbone. The ratio $\tau_1(\text{OACF})/\tau_2(\text{OACF}) \equiv A_r$ is a measure of the anisotropy of the relaxation.[36] A value of $A_r = 3$ indicates isotropic rotational motion of the vector (equal probability for motion in any direction) while a value other than three indicates anisotropy in the relaxation process. For example, in-plane motion of a vector results in relatively fast decay of $P_1(t)$ yielding $A_r < 3$ while motion in a conical section results in relatively fast decay of $P_2(t)$ yielding $A_r > 3$.

The C−H and statistical segment vector anisotropy ratios shown in Figure 3a indicate that vector reorientational dynamics become monotonically more isotropic with dilution. The decreasing solution viscosity (see below) and chain density with dilution allow for more isotropic motions of the vectors as local chain motions become less restricted to lie along the local chain backbone. This restriction results in $A_r < 3$ for C−H vectors (largely perpendicular to the local chain backbone) and $A_r > 3$ for statistical segments (largely along the backbone) and engenders cooperative conformational motions. A similar "matrix memory" effect was observed for polyethylene when the dynamics of melt chains were compared to those of isolated chains,[37] where we found that the extent of cooperative conformational transitions was greater in the melt compared to isolated chains. Decreasing cooperativity with dilution is probably important in determining the efficacy of conformational transitions in relaxing the C−H and statistical segment vectors, leading, in conjunction with the decreasing viscosity, to the decrease in correlation time for these vectors with dilution for $w_p < 0.78$ despite the continued decrease in the rate of conformational transitions.

In summary, the maxima in τ(OACF) in the range $w_p = 0.78-0.90$ are likely the result of a combination of a decreasing rate of conformational transitions (common to the mechanism for the relaxation of TACFs) and an increase in solution viscosity in this range. The reduction in τ(OACF) with dilution for $w_p < 0.78$ is largely due to the influence of a decreasing solution viscosity, as discussed below, and decreasing cooperativity in conformational dynamics leading to more efficacious (isotropic) segmental relaxation. Hence, the increasing β in this composition range for τ(the OACFs) seems to reflect primarily the influence decreasing cooperativity in conformational transitions on segmental dynamics with dilution while for the TACFs it reflects the influence of decreased conformational dynamic heterogeneity.

V. Intermediate Incoherent Dynamic Structure Factor

A. *I*(*q*,*t*). Monitoring the intermediate incoherent structure factor $I(q,t)$ resulting from motion of PEO hydrogen atoms provides a convenient way of studying polymer chain dynamics on various length scales. $I(q,t)$ for an isotropic sample is given as[38]

$$I(q,t) = \left\langle \frac{\sin[qr(t)]}{qr(t)} \right\rangle \tag{7}$$

where q is the magnitude of the momentum transfer vector, $r(t)$ is the displacement of an atom during time t, and $\langle\ \rangle$ denotes an ensemble average over all hydrogen atoms. Figure 5 shows $I(q,t)$ for PEO/water solutions for $q = 1.57$ Å^{-1} corresponding to the position of the first

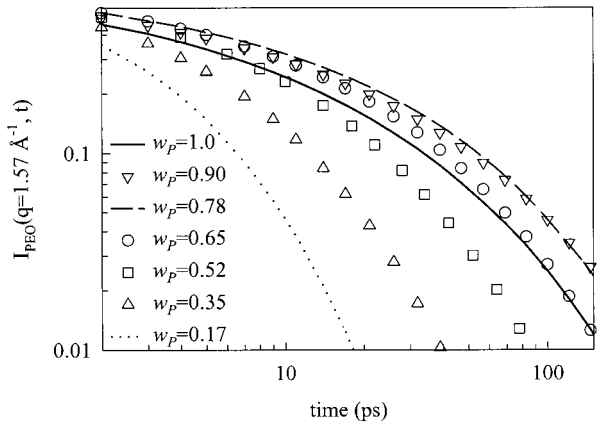

Figure 5. PEO intermediate incoherent structure factor I (q = 1.57 Å^{-1}, t) for PEO/water solutions.

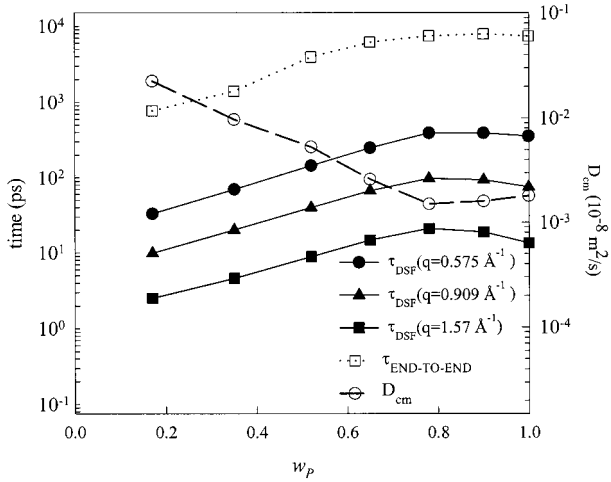

Figure 6. Autocorrelation times $\tau_{DSF}(q)$ and the end-to-end vector autocorrelation time $\tau_{END-TO-END}$ as a function of solution composition. Also shown is the self-diffusion coefficient for PEO (D_{cm}).

maximum of the static structure factor in the pure PEO melt. Examination of the concentration dependence of $I(q,t)$ reveals that the dynamics of PEO slow on this length scale ($2\pi/q \approx 4$ Å) with the initial addition of water compared to the pure melt. The slowest polymer dynamics are observed in the composition range w_p = 0.78−0.9. The correlation times $\tau_{DSF}(q)$ (DSF = dynamic structure factor) for the incoherent dynamic structure factor, obtained as the time integral of KWW fits to eq 7, are shown in Figure 6 as a function of composition for a wide range of momentum transfers. These momentum transfers cover length scales from that of the monomer to greater than that of the radius of gyration of the chains, indicating that the initial slowing down of polymer dynamics with addition of water occurs on all length scales but is greater for smaller length-scale motions. In contrast, the dramatic decrease in relaxation time with further dilution is greatest for largest length-scale motions (see also Figure 9).

B. Deviation of Atom Displacements from Gaussian Behavior. Non-Gaussian behavior for atom displacements slows down the decay of the dynamic structure factor compared to a system with the same mean-square, but Gaussian distributed, displacements.[39] It is known that molecular motion on short time scales (ballistic regime and harmonic) and on long time scales (diffusive) is Gaussian.[40] On intermediate time scales where the dynamics of individual conformations dominate, molecular motion in polymers is typically non-Gaussian.[39,41] It is conceivable that the greater heterogeneity in conformational dynamics observed in the composition range w_P = 0.78−0.9 may lead to greater non-Gaussianity in polymer motions, thereby accounting for the maxima in $\tau_{DSF}(q)$ in this composition range. The second cumulant provides a measure of the deviation of atom displacements from Gaussian behavior and is given by

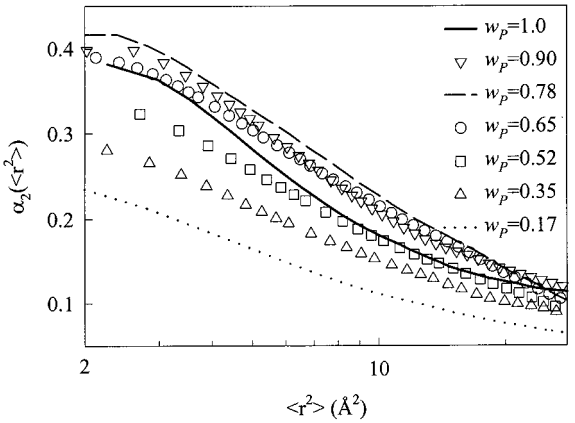

Figure 7. Non-Gaussianity parameter for PEO hydrogen atom displacements $\alpha_2(\langle r^2 \rangle)$ as a function of solution composition.

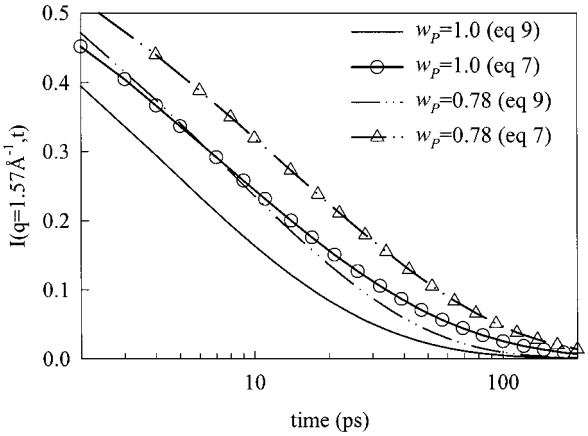

Figure 8. PEO intermediate incoherent structure factor $I(q$ = 1.57 Å^{-1}, t) from direct calculations (eq 7) and from the Gaussian approximation (eq 9) for PEO/water solutions.

$$\alpha_2(\langle r^2(t) \rangle) = \frac{3\langle r^4(t) \rangle}{5\langle r^2(t) \rangle} - 1 \qquad (8)$$

where $\langle r^n(t) \rangle$ is the nth moment of the displacement distribution of hydrogen atoms during time t. $\alpha_2(\langle r^2 \rangle)$ for PEO/water is shown in Figure 7. Note that $\alpha_2(\langle r^2 \rangle)$ is consistently larger for $w_p \approx 0.78$ than for the PEO melt and dilute solutions. In Figure 8 we compare $I(q,t)$ (q = 1.57 Å^{-1}) from simulation and from that obtained using the Gaussian approximation[40]

$$I^{GAUSS}(q,t) = \exp[-q^2\langle r^2(t) \rangle/6] \qquad (9)$$

The difference between $I^{GAUSS}(q,t)$ and $I(q,t)$ is due to non-Gaussianity in hydrogen displacements. While non-Gaussian effects clearly influence the decay of $I(q,t)$, they are not primarily responsible for the relatively slow decay seen in $I(q,t)$ for $w_p \approx 0.78$ compared to the pure melt. For q = 1.57 Å^{-1} non-Gaussian effects appear to

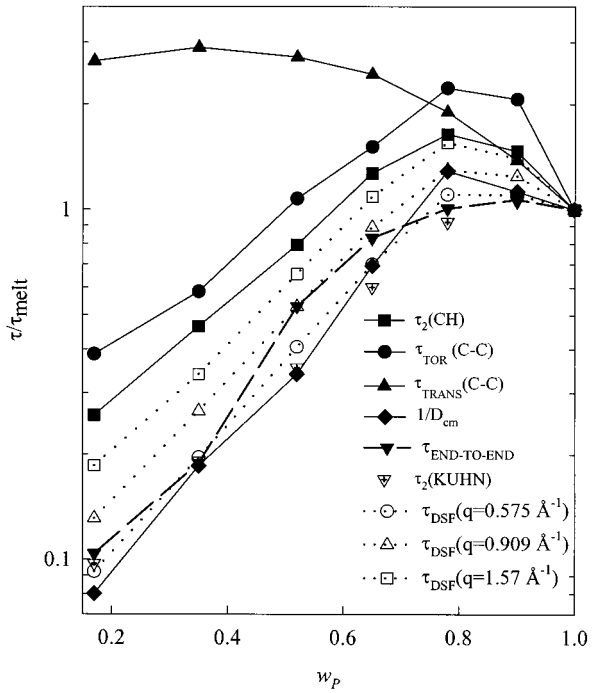

Figure 9. Ratio of the mean conformational transition and autocorrelation times to those in pure PEO melt as a function of solution composition.

account for about $^1/_3$ of the increase in τ_{DSF} at $w_p = 0.78$ compared to the pure melt.

VI. Global Chain Dynamics

The self-diffusion coefficient (D_{cm}) for the PEO chains is given as

$$D_{cm} = \lim_{t\to\infty} \frac{\langle \mathbf{R}^2_{cm}(t)\rangle}{6t} \tag{10}$$

where $\langle \mathbf{R}^2_{cm}(t)\rangle$ is the mean-square displacement of the chain center of mass during time t. The self-diffusion coefficient for PEO chains in PEO/water solutions is shown in Figure 6. Also shown is the autocorrelation time $\tau_{END-TO-END}$ for the end-to-end vector reorientation, given by eq 3a, where the unit vector corresponds to the chain end-to-end vector. Values of $\tau_{END-TO-END}$ were determined from the time integration of KWW fits to eq 3a for the end-to-end vector OACF. Polymer solution theory directly relates the end-to-end vector relaxation to the solution viscosity.[42] We observe a minimum in the PEO self-diffusion coefficient and a maximum in $\tau_{END-TO-END}$ in the composition range $w_p = 0.78-0.90$. This is consistent with the behavior of $I(q,t)$ for small q (large length scales) discussed above. We also note that the PEO self-diffusion coefficient $D_{cm} = 0.023$ Å^2/ps at 298 K and $w_p = 0.52$ from our MD simulations of PEO(MW=530)/H_2O solutions compares favorably with the $D_{PEO} = 0.017$ Å^2/ps from QENS measurements[43] on PEO(MW=600)/D_2O at 303 K at $w_p = 0.53$.

Figure 9 shows the relaxation times for all the processes discussed (conformational, segmental, and global chain) scaled by their corresponding value in the pure melt. The disconnect between the relaxation processes and the mean rate of conformational transitions can clearly be seen. The maxima in relaxation time for processes on all length scales in the composition range $w_p = 0.78-0.90$ can also be clearly seen. Those processes that involve the largest length-scale motions (self-diffusion, $I(q,t)$ for small q) more closely follow the behavior the solution viscosity ($\tau_{END-TO-END}$). The composition dependence of the statistical segment relaxation also closely resembles that of the viscosity, indicating the importance of large length-scale motions in the reorientation of the statistical segment for the relatively short chains considered here. For relaxation processes that involve more local motions, namely the C-H vector OACFs and $I(q,t)$ for large q, the increase in dynamics with dilution is significantly less pronounced than is seen for the larger length-scale motions. On these length scales the decreasing/saturation of conformational dynamics with dilution appears to be more strongly manifested.

VII. Conclusions

Our simulations reveal that addition of a relatively minor amount of water to a PEO melt dramatically affects conformational, segmental, and global dynamics. The influence of water on polymer dynamics on the various length scales can be summarized as follows. Most fundamentally, water slows the rate of conformational transitions, an effect that sets in rapidly with initial dilution but saturates at $w_p \approx 0.5$. At this composition, PEO−water hydrogen bonding is nearly saturated, and the first PEO hydration shell is largely formed. Second, water initially leads to an increase in the heterogeneity of the rates of conformational transitions, with a maximum in the range $w_p = 0.78-0.90$, followed by decrease in heterogeneity with further dilution. This is probably a consequence of the structural heterogeneity that occurs in concentrated solutions relative to either the pure melt or dilute solution—dihedrals in the melt all experience a polymer environment and in dilute solution an aqueous environment, while in concentrated solution there is a distribution of local environments. This increase in the heterogeneity in conformational dynamics for concentrated solutions seems to lead to a maximum in non-Gaussianity in polymer atom displacements in this composition range, an effect that is partially responsible for the maximum in τ_{DSF}. Third, water leads to a monotonic decrease in segmental motion anisotropy. This effect is probably associated with an increase the efficacy of conformational motions to bring about local orientational decorrelation, such as decay of the C−H vector OACF, with dilution. Finally, water initially leads to an increase and then a dramatic decrease in solution viscosity and hence the longer polymer relaxation times.

In general, the maximum in relaxation time in the composition range $w_p = 0.78-0.90$ is most pronounced for more localized motions and the dramatic decrease in relaxation time with further dilution is most pronounced for larger length-scale motions. We know that water clustering is quite strong in solutions in the composition range $w_p = 0.78-0.90$ and that hydrogen bonding saturates for $w_p < 0.5$.[24] In future papers we will consider the role of water−ether and water−water hydrogen bonding on PEO dynamics on all length scales and present a detailed normal-mode analysis of PEO dynamics in aqueous solution as a function of composition.

Acknowledgment. The authors are indebted to the National Science Foundation−Division of Materials Research for support through NSF CAREER award

DMR 0076306. An allocation of computer time from the center for the High Performance Computing at the University of Utah is gratefully acknowledged. We also thank R. Boyd and F. Trouw for helpful discussions.

References and Notes

(1) Saeki, S.; Kuwahara, N.; Nakata, M.; Kaneko, M. *Polymer* **1976**, *17*, 685.
(2) Tjerneld. F. In *Poly(Ethylene Glycol) Chemistry: Biotechnical and Biomedical Applications*; Harris, J. M., Ed.; Plenum Press: New York, 1992; p 85.
(3) McPherson, A. *Methods Enzymol.* **1985**, *114*, 112.
(4) McPherson, A. *J. Cryst. Growth* **1991**, *110*, 1.
(5) Cudney, B.; Patel, S. *Acta Crystallogr.* **1994**, *D50*, 414.
(6) Harris, J. M. In *Poly(Ethylene Glycol) Chemistry: Biotechnical and Biomedical Applications*; Harris, J. M., Ed.; Plenum Press: New York, 1992; p 1.
(7) Andrade, J. D.; Hlady, V.; Jeon, S. I. *Polym. Mater. Sci. Eng.* **1993**, *69*, 60.
(8) Asakura, S.; Oosawa, F. *J. Polym. Sci.* **1958**, *33*, 183.
(9) Poon, W. C. K.; Pirie, A. D.; Haw, M. D.; Pusey, P. N. *Physica A* **1997**, *235*, 110.
(10) Rex, S.; Zuckermann, M. J.; Lafleur, M.; Silvius, J. R. *Biophys. J.* **1998**, *75*, 2900.
(11) Evans, E.; Rawicz, W. *Phys. Rev. Lett.* **1997**, *79*, 2379.
(12) Albertsson, P. *Aqueous Biphasic Separations*; Rogers R. D., Eiteman, M. A., Eds.; Plenum Press: New York, 1995; p 21.
(13) Bedrov, D.; Pekny, M.; Smith, G. D. *J. Phys. Chem. B* **1998**, *102*, 996.
(14) Bedrov, D.; Borodin, O.; Smith, G. D. *J. Phys. Chem. B* **1998**, *102*, 5683.
(15) Bedrov, D.; Borodin, O.; Smith, G. D. *J. Phys. Chem. B* **1998**, *102*, 9565.
(16) Bedrov, D.; Smith, G. D. *J. Phys. Chem. B* **1999**, *103*, 3791.
(17) Bedrov, D.; Borodin, O.; Smith, G. D.; Trouw, F.; Mayne, C. *J. Phys. Chem. B* **2000**, *104*, 5151.
(18) Liu, H.; Müller-Plathe, F.; van Gunsteren, W. F. *J. Chem. Phys.* **1995**, *102*, 1722.
(19) Engkvist, O.; Åstrand, P.; Karlström, G. *J. Chem. Phys.* **1996**, *100*, 6950.
(20) Williams, D. J.; Hall, K. B. *J. Phys. Chem.* **1996**, *100*, 8224.
(21) Tasaki, K. *J. Am. Chem. Soc.* **1996**, *118*, 8459.
(22) Engkvist, O.; Karlström, G. *J. Chem. Phys.* **1997**, *106*, 2411.
(23) Borodin, O.; Trouw, F.; Bedrov, D.; Smith, G. D. Manuscript in preparation.
(24) Smith, G. D.; Bedrov, D.; Borodin, O. *J. Am. Chem. Soc.* **2000**, *122*, 9548.
(25) Smith, G. D.; Bedrov, D.; Borodin, O. *Phys. Rev. Lett.* **2000**, *85*, 5583.
(26) Smith, G. D.; Jaffe, R. L.; Yoon, D. Y. *J. Phys. Chem.* **1993**, *97*, 12752.
(27) Jorgensen, W. L.; Chandrasekhar, J.; Madura, J. D.; Impey, R. W.; Klein, M. *J. Chem. Phys.* **1983**, *79*, 926.
(28) Allen, M. P.; Tildesley, D. J. *Computer Simulation of Liquids*; Oxford University Press: New York, 1987.
(29) Ryckaert, J. P.; Ciccotti, G.; Berendsen, H. J. C. *J. Comput. Phys.* **1977**, *23*, 327.
(30) Tuckerman, M.; Berne, B. J.; Martyna, G. J. *J. Chem. Phys.* **1992**, *97*, 1990.
(31) Tuckerman, M.; Berne, B. J.; Martyna, G. J. *J. Chem. Phys.* **1991**, *94*, 6811.
(32) Borodin, O.; Smith, G. D. *Macromolecules* **2000**, *33*, 2273.
(33) Smith, G. D.; Yoon, D. Y.; Wade, C. G.; O'Leary, D.; Chen, A.; Jaffe, R. L. *J. Chem. Phys.* **1997**, *106*, 3798.
(34) Smith, G. D.; Borodin, O.; Bedrov, D.; Paul, W.; Qiu, X. H.; Ediger, M. D. *Macromolecules*, in press.
(35) Ediger, M. D. *Annu. Rev. Phys. Chem.* **2000**, *51*, 99.
(36) Perico, A.; Guenza, M. *J. Chem. Phys.* **1985**, *83*, 3103.
(37) Smith, G. D.; Jaffe, R. L.; Yoon, D. Y. *Macromolecules* **1995**, *28*, 5897.
(38) Higgins, J. S.; Benoît, H. *Polymers and Neutron Scattering*; Oxford University Press: Oxford, 1996.
(39) Smith, G. D.; Paul, W.; Monkenbusch, M.; Richter, D. *J. Chem. Phys.* **2001**, *114*, 4285.
(40) McQuarrie, D. A. *Statistical Mechanics*; Harper & Row: New York, 1976.
(41) Smith, G. D.; Paul, W.; Yoon, D. Y.; Zirkel, A.; Hendricks, J.; Richter, D.; Schober, H. *J. Chem. Phys.* **1997**, *107*, 4751.
(42) Doi, M.; Edwards, S. F. *The Theory of Polymer Dynamics*; Oxford University Press: Oxford, 1986.
(43) Crupi, V.; Magazu, S.; Majolino, D.; Migliardo, P.; Wanderlingh, U.; Kagunya, W. W. *Physica B* **1998**, *241*−*243*, 979.

MA010038B